Anomalous Diffusion in Living Yeast Cells

Iva Marija Tolić-Nørrelykke,[1,*] Emilia-Laura Munteanu,[1] Genevieve Thon,[2]
Lene Oddershede,[1] and Kirstine Berg-Sørensen[1]
[1]*The Niels Bohr Institute, Blegdamsvej 17, DK-2100 Copenhagen Ø, Denmark*
[2]*Institute of Molecular Biology, Øster Farigmagsgade 2A, DK-1353 Copenhagen K, Denmark*
(Received 31 July 2003; published 13 August 2004)

The viscoelastic properties of the cytoplasm of living yeast cells were investigated by studying the motion of lipid granules naturally occurring in the cytoplasm. A large frequency range of observation was obtained by a combination of video-based and laser-based tracking methods. At time scales from 10^{-4} to 10^{2} s, the granules typically perform subdiffusive motion with characteristics different from previous measurements in living cells. This subdiffusive behavior is thought to be due to the presence of polymer networks and membranous structures in the cytoplasm. Consistent with this hypothesis, we observe that the motion becomes less subdiffusive upon actin disruption.

DOI: 10.1103/PhysRevLett.93.078102 PACS numbers: 87.80.Cc, 05.40.Jc, 46.35.+z

The unravelling of the complex machinery of a living cell is currently receiving substantial attention [1]. An important constituent of this machinery is the cytoskeleton which has a key role in many cell functions, such as regulation of cell shape, cell motility, division, and intracellular transport. Networks of cytoskeletal polymers have been studied *in vitro* [2–5], and living cells have been addressed through microrheology experiments [6–9]. Still, the physical properties of the *in vivo* cytoskeleton remain to a large extent unknown.

In this work, we probe the mechanics within a living cell on the nanometer scale. We study the fission yeast *Schizosaccharomyces pombe,* which is characterized by a stiff cell wall that is responsible for the cell shape and resistance to deformation. Thus, the mechanics of the cells studied here differ from that of the soft cells used in previous microrheology studies [8,9].

In order to investigate the viscoelastic properties of the cytoplasm and the contribution of the cytoskeleton to those properties, we monitored the motion of small lipid granules that occur naturally in the cytoplasm. The granules are highly refractive, almost spherical, and filled with lipids [10]. The granules vary in size with a typical diameter of ~300 nm, whereas the whole cell is ~12 μm long and 4 μm wide. The granules are embedded in the cytoskeleton, which consists of a sparse microtubule network [11] and actin filaments [12]. Fluctuations of a granule position may be limited by the polymer networks of the cytoskeleton. We therefore performed experiments in both intact cells and cells in which the actin network was disrupted. In light microscopy the granules appear as small black spheres (Fig. 1) that move in a seemingly random fashion. By combining optical tweezers and video-based image analysis, a wide frequency range of observation was covered, from 0.01 Hz to above 10 kHz.

Biological specimen.—S. pombe cells were grown for 12–14 hours at 30 °C on plates containing AA medium [13]. The cells were then transferred to a perfusion chamber in a liquid medium where they firmly adhered in a monolayer to a poly-L-lysine-covered glass coverslip. This immobilization assured easy observation and minimized drift. Experiments were performed on cells in interphase. In order to disrupt actin filaments, the cells were treated with 50 μM Cytochalasin D (CD) in 1% dimethyl sulfoxide (DMSO) for 15–60 minutes. Control cells were treated with 1% DMSO for 15–60 min.

Optical tweezers (OT) experiments.—The optical trap was formed by a focused laser beam from a Nd:YVO_4 laser within an inverted microscope [14]. A granule inside a cell was optically trapped in a very weak laser trap with a trap stiffness of $\sim 5 \times 10^{-3}$ pN/nm, and its motion was detected by a Si-PIN quadrant photodiode in the back focal plane. This technique is nearly noninvasive; we estimated the laser power in the sample to be ~20 mW and hence the heating effect of the trap <1 °C [15]. The sampling rate was 22 kHz and the spatial resolution 1–2 nm.

Multiple particle tracking (MPT).—The motion of granules in the cell was also detected by video-based image analysis with a sampling rate of 25 frames/s. A correlation algorithm was used to determine the displacement of individual granules at subpixel resolution [16]. The spatial resolution of this method was <10 nm, esti-

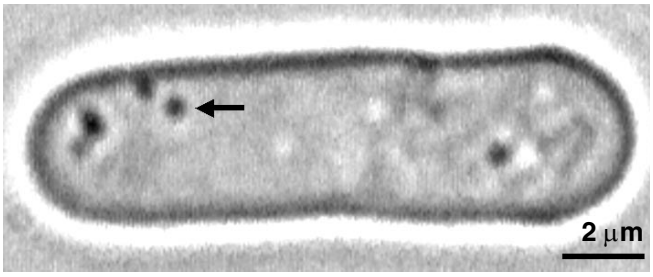

FIG. 1. Image of a fission yeast cell. Small black spheres are lipid granules in the cytoplasm (arrow).

mated as the variance of the distance between two immobilized polystyrene spheres of a size similar to that of a granule. In order to correct for the possible movement of the frame of reference (the cell or the whole chamber), the displacement of the outline of the cell was subtracted from the displacement of the granule. During a typical MPT measurement of 2–3 min, a granule moved 100–300 nm, whereas the whole cell moved about 20 nm. Both small and large excursions of the granules could be tracked.

Analysis of motion.—In order to classify the motion of a particular granule, time series of its position $\vec{r}(t) = (x(t), y(t))$ were recorded. From the measured positions we calculated the mean squared displacement (MSD), $\langle|\Delta\vec{r}(t)|^2\rangle$, where t is now time lag. The average was taken over time within a single trajectory. Evaluation of a "distinct mean squared displacement" based on two-point microrheology [17] agreed with the normal MSD for an example of four granules in one cell, indicating that the normal MSD was not affected by variations in the granule shape and size, or by the inhomogeneity of the medium.

Theoretically, the mean squared displacement of a diffusing particle varies with time as

$$\langle|\Delta\vec{r}(t)|^2\rangle \propto t^{\alpha}, \tag{1}$$

where the exponent α distinguishes the type of diffusion encountered; $\alpha = 1$ indicates normal Brownian diffusion, $\alpha < 1$ indicates subdiffusion, and $\alpha > 1$ indicates superdiffusion [18,19].

The Fourier transform of the position obtained by OT, $(\tilde{x}(f), \tilde{y}(f))$, leads to the power spectra of the granule's position $(P_x(f), P_y(f))$ where $P_x(f) \equiv \langle|\tilde{x}(f)|^2\rangle$ and $P_y(f) \equiv \langle|\tilde{y}(f)|^2\rangle$. If the motion of a granule is described by a generalized Langevin equation with a time-dependent friction coefficient, the power law variation $\langle|\Delta\vec{r}(t)|^2\rangle \propto t^{\alpha}$ results in a similar power law of the power spectra $(P_x(f), P_y(f))$:

$$P_i(f) = kf^{-(1+\alpha)}; \qquad i = x, y, \tag{2}$$

where the parameters α and k are fitting parameters. The recorded experimental power spectrum differs from $P_i(f)$ of Eq. (2) due to artifacts of the data-acquisition system. By accounting for those, we can achieve a precise determination of α using all data out to the Nyquist frequency: In the high frequency range, the position detection system acts as a filter [20]. Also, other filters in the data-acquisition electronics and aliasing must be taken into account [21]. In order to extract statistical errors on the parameters obtained, we fitted to "blocked" data points with known standard deviation [21], using a modification of the computer codes from Ref. [22].

For the granule in water, the power spectrum shows a corner frequency (f_c) due to the optical trapping, which was found to be within the fitting frequency range (200 Hz–11 kHz). The fit to the data of the granule in water had four free parameters: f_c, α, k, and the effective filtering frequency of the data-acquisition system (f_{da}). For granules inside the cell, f_c was found below the fitting range, at frequencies <10 Hz. The fit to the data of the granule inside the cell thus had only three free parameters: α, k, and f_{da}. In the results presented below, the value of α obtained for a population of granules is given as mean value $\pm$ standard error on the mean.

Results.—As a control, granules that diffused out of a cell lysed with enzymes were analyzed. Each of these granules was optically trapped in water and was expected to exhibit normal Brownian motion in the trap. This was verified, as we found $\alpha = 1.004 \pm 0.0003$ ($N = 23$ granules). In contrast, optical tweezers measurements on granules inside the living cells gave $\alpha = 0.737 \pm 0.003$ ($N = 266$). This value of α is close to the exponent of a particle performing subdiffusive motion within a semiflexible polymer network [23,24]. Figure 2 shows power spectra of OT data both from a granule diffusing in water and from a granule moving inside a living cell. The difference in slope above 1 kHz, and thus in α, is clearly visible.

Figure 3 shows $\langle|\Delta\vec{r}(t)|^2\rangle$ as a function of time for granules analyzed by OT (short-time-lag part of the data) and by MPT (long-time-lag part of the data). The two independent experimental measurement procedures do not overlap in the frequency interval. However, Fig. 3 indicates that the MPT data are a reasonable extension of the OT data. A dominant slope of order 0.75 shows that a typical granule performs subdiffusion over a large range of time scales. At all time scales the exponent α is, to a

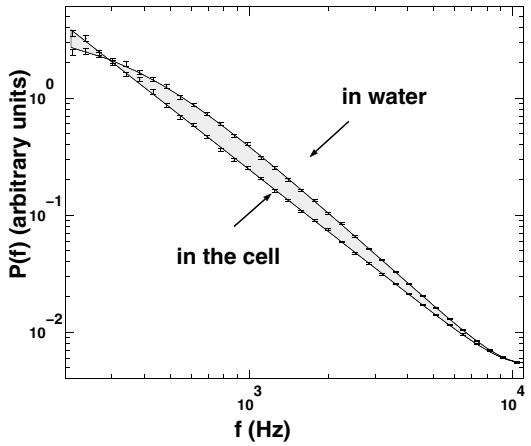

FIG. 2. Power spectra of thermal motion of a free granule in water (marked "in water") and a granule inside the cell (marked "in the cell"). The data points shown were blocked with equal bin width on the logarithmic frequency axis. Error bars are so small that they are not visible at high frequencies. The lines show the fit of the theory to the data (see text) from $f_{\mathrm{min}} = 200$ Hz to the Nyquist frequency, 11 kHz. The fit to the data of the granule inside the cell gave an exponent $\alpha = 0.762 \pm 0.006$. For the granule in water, the fit yielded $\alpha = 1.00 \pm 0.01$.

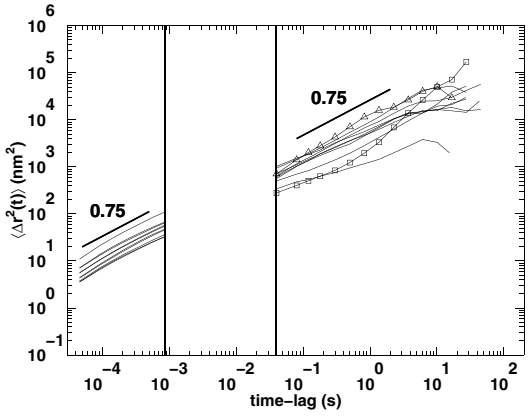

FIG. 3. Mean squared displacement, $\langle |\Delta \vec{r}(t)|^2 \rangle$, of granules as a function of time lag. The short-time part of the data was obtained by OT ($N = 10$ randomly chosen granules), whereas the long-time part was obtained by MPT (other ten granules). Lines with a slope of 0.75 are drawn to guide the eye. Lines with symbols show examples of different types of motion: normal diffusion (Δ), subdiffusion with a plateau (●), and directed motion (□).

good approximation, normally distributed in a population of granules, as summarized in Table I.

To address the origin of the observed subdiffusive motion, we performed experiments in which actin filaments in living cells were disrupted by CD. If actin filaments restrict the motion of the granules, disruption of the actin network should induce a shift in the granule motion towards normal diffusion, which can be measured by an increase in α. In OT measurements on cells treated with CD, the exponent α was found to be $\alpha = 0.755 \pm 0.006$ ($N = 52$). The value of α measured in the same set of cells before treatment was $\alpha = 0.734 \pm 0.004$ ($N = 59$, a subset of $N = 266$ from Table I, first row). These values of α come from the fits with a goodness of fit [25] larger than 10%, which was the case for 89.9% of the total fits. The goodness of fit decreased substantially when the data were fitted with a fixed $\alpha = 0.75$, suggesting that it is possible to discern small differences in α; see [26]. A student's t test [25] showed that the untreated and the CD-treated sample are significantly different, i.e., that they could have the same mean with a probability $p < 0.01$. Since cell-to-cell variation in exponents is rather large, we also compared the mean exponent for each cell before and after the CD treatment using a paired t test [25], which yielded the same result ($p < 0.01$). Control experiments where cells were treated similarly but without CD did not show a significant change in α ($p = 0.4$). The increase in α following CD treatment is consistent with findings in [8,27]. No anisotropy with respect to the cell axes was detectable in the motion of the lipid granules either before or after the treatment with CD. When the cells are placed in water for a prolonged period, vacuoles fuse in response to osmotic stress [28]. This was utilized to perform an additional control measurement: We measured $\alpha = 0.99 \pm 0.02$ and 0.98 ± 0.02 in cells placed in water. This corresponds to a normal diffusion of the granules, presumably within a fluid-filled vacuole.

TABLE I. Distribution of the exponent α in three different intervals of time lag. The value of α was found by fitting a Gaussian to the histogram of α. The 46 MPT granules are a subset of the 52 MPT granules, whereas the 266 OT granules are an independent set.

Method	Time interval (s)	Total count	α
OT	10^{-4}–10^{-3}	266	0.737 ± 0.003
MPT	0.1–1	52	0.68 ± 0.02
MPT	1–10	46	0.70 ± 0.03

For a particle embedded in a semiflexible polymer network, $\langle |\Delta \vec{r}(t)|^2 \rangle$ is expected to display a plateau ($\alpha \simeq 0$) at long-time lags, where the particle is elastically trapped in the network [23]. Also, the confinement of a granule between larger cell organelles would result in a plateau in $\langle |\Delta \vec{r}(t)|^2 \rangle$. For $N = 8$ granules ($\sim 15\%$), we observed a flattening of the MSD curve, consistent with the onset of a plateau at times 1–10 s, e.g., Fig. 3 (●). There was a large variation between individual granules with respect to whether they showed a MSD plateau or not at the time scale of our experiments, and a 10-fold variation in the plateau value among those that did. This variation could be due to a variation in the granule size and in the local properties of the cytoplasm, i.e., filament length and density, as well as the density of cross-linkers [29].

At the longest time lags, the filaments of the network disentangle and the system behaves like a viscous fluid. This fluid behavior of the cytoplasm with $\alpha \simeq 1$ was observed in $N = 6$ granules ($\sim 12\%$), which exhibited normal diffusion, e.g., Fig. 3 (△). Furthermore, $N = 3$ granules ($\sim 6\%$) performed superdiffusion for more than one decade of time. This superdiffusive motion could be caused by local cytoplasmic flow, by molecular motors, or by polymerization forces.

Discussion.—The observed subdiffusive motion of granules in the cytoplasm of a living yeast cell is probably caused by the granule being embedded in a protein polymer network, or mechanically coupled to other structures with similar bending modes, e.g., membrane stacks or vesicles inside the cell. The value $\alpha \simeq 0.75$ found here in a large window of time lags is similar to that measured in the cytoplasm of higher eukaryotic cells for small time lags ($\alpha \simeq 0.70$) [8] or for large time lags [7]. But also significantly smaller values have been found in higher eukaryotic cells: For beads attached to the surface of cells, $\alpha \simeq 0.17$ [27], and for granules in the cytoplasm, $\alpha \simeq 0.2$ at large time lags [8]. This indicates that the viscoelastic landscape of the yeast cell may be quite different from that of higher eukaroytic cells and more consistent with the physical properties of *in vitro* actin networks [2]. Since cells with disrupted actin filaments

showed only a slight increase in α, other cytoplasmic structures, such as intracellular membranes and other polymer networks, are suggested as the main causes of the restriction of motion. Further experiments to explore the origin of the different types of motion found here could include blocking of adenosine-triphosphate-driven activity to test for possible active transport by molecular motors.

For an object embedded in a complex fluid, a generalized Stokes-Einstein equation relates $\langle|\Delta\vec{r}(t)|^2\rangle$ to the storage modulus G' and the loss modulus G'' of the bulk complex fluid [30]. For this approach to be valid, the particle must be rigid and spherical, which is satisfied by the lipid granules, and the medium must be well approximated by an infinite isotropic viscoelastic continuum, where inertia can be neglected. The infinity condition does not hold here because of the existence of the cell wall at a distance of 1–10 particle diameters away from the particles. Further, corrections due to the two-fluid medium composed of a protein network and the solvent may be needed at low frequencies [31], as well as corrections due to the crossover between affine and nonaffine deformations [32,33]. However, using this approach on a typical granule that does not exhibit superdiffusion and is more than 1 μm away from the cell wall yields moduli $G'(f)$ and $G''(f)$ that both vary as $f^{0.75}$ for over five frequency decades. The loss modulus $G''(f)$ dominates for $f > 0.2$ Hz, $G''(f) \simeq 1$ Pa$(f/1\ \text{Hz})^{0.75}$.

Summary.—The viscoelastic properties of the cytoplasm in living yeast cells were studied in a large frequency window. The mean squared displacement of lipid granules increased with time roughly as $t^{0.75}$ from below 10^{-4} to 100 s, indicating an unvarying subdiffusive behavior over a large range of time scales, in contrast to earlier observations in living cells [8]. At larger time lags examples of other types of motion, such as confined and superdiffusive motion, were observed, reflecting a part of the complex dynamics of a living cell.

We thank Inga Sig Nielsen for help with cell preparation, and Henrik Flyvbjerg, Ralf Metzler, Ben Fabry, and Simon F. Tolić-Nørrelykke for a critical reading of the manuscript. This work was supported by the Danish Research Councils, NATO, the Lundbeck Foundation, and the BIOP graduate school.

*Permanent address: Rugjer Bošković Institute, Bijenička 54, HR-10000 Zagreb, Croatia.

[1] Deepa Nath, Nature insight: Cytoskeleton. Nature **422**, 739 (2003).
[2] F. Amblard *et al.*, Phys. Rev. Lett. **77**, 4470 (1996).
[3] F. Gittes *et al.*, Phys. Rev. Lett. **79**, 3286 (1997).
[4] A. Palmer *et al.*, Biophys. J. **76**, 1063 (1999); Y. Tseng and D. Wirtz, Biophys. J. **81**, 1643 (2001); M. Dichtl and E. Sackmann, Proc. Natl. Acad. Sci. U.S.A. **99**, 6533 (2002).
[5] I. Y. Wong *et al.*, Phys. Rev. Lett. **92**, 178101 (2004).
[6] A. R. Bausch, W. Möller, and E. Sackmann, Biophys. J. **76**, 573 (1999).
[7] A. Caspi, R. Granek, and M. Elbaum, Phys. Rev. Lett. **85**, 5655 (2000).
[8] S. Yamada, D. Wirtz, and S. Kuo, Biophys. J. **78**, 1736 (2000).
[9] Y. Tseng, T. P. Kole, and D. Wirtz, Biophys. J. **83**, 3162 (2002).
[10] C. F. Robinow and J. S. Hyams, in *Molecular Biology of the Fission Yeast*, edited by A. Nasim, P. Young, and B. F. Johnson (Academic Press, Inc., San Diego 1989), pp. 273–330.
[11] I. M. Hagan, J. Cell Sci. **111**, 1603 (1998).
[12] J. R. J. Pelham and F. Chang, Nature Cell Biol. **3**, 235 (2001).
[13] M. Rose, F. Winston, and P. Hieter, *Methods in Yeast Genetics: A Laboratory Course Manual* (Cold Spring Harbor Laboratory Press, Cold Spring Harbor, NY, 1990).
[14] L. Oddershede *et al.*, Probe Microsc. **2**, 129 (2001).
[15] E. J. G. Peterman, F. Gittes, and C. F. Schmidt, Biophys. J. **84**, 1308 (2003).
[16] I. M. Tolić-Nørrelykke *et al.*, Am. J. Physiol. Cell Physiol. **283**, C1254 (2002).
[17] J. C. Crocker *et al.*, Phys. Rev. Lett. **85**, 888 (2000).
[18] M. J. Saxton and K. Jacobson, Annu. Rev. Biophys. Biomol. Struct. **26**, 373 (1997).
[19] R. Metzler and J. Klafter, Phys. Rep. **339**, 1 (2000).
[20] K. Berg-Sørensen *et al.*, J. Appl. Phys. **93**, 3167 (2003).
[21] K. Berg-Sørensen and H. Flyvbjerg, Rev. Sci. Instrum. **75**, 594 (2004).
[22] I. M. Tolić-Nørrelykke, K. Berg-Sørensen, and H. Flyvbjerg, Comput. Phys. Commun. **159**, 225 (2004).
[23] F. Gittes and F. C. MacKintosh, Phys. Rev. E **58**, R1241 (1998).
[24] D. C. Morse, Phys. Rev. E **58**, R1237 (1998).
[25] W. H. Press, B. P. Flannery, S. A. Teukolsky, and W. T. Vetterling, *Numerical Recipes. The Art of Scientific Computing* (Cambridge University Press, Cambridge, 1986).
[26] See EPAPS Document No. E-PRLTAO-93-036432 for details on the fits and the random walker simulations. A direct link to this document may be found in the online article's HTML reference section. The document may also be reached via the EPAPS homepage (http://www.aip.org/pubservs/epaps.html) or from ftp.aip.org in the directory /epaps/. See the EPAPS homepage for more information.
[27] B. Fabry *et al.*, Phys. Rev. Lett. **87**, 148102 (2001).
[28] N. Bone *et al.*, Curr. Biol. **8**, 135 (1998).
[29] J.-Q. Wu, J. Bähler, and J. R. Pringle, Mol. Biol. Cell **12**, 1061 (2001).
[30] T. G. Mason and D. A. Weitz, Phys. Rev. Lett. **74**, 1250 (1995).
[31] A. J. Levine and T. C. Lubensky, Phys. Rev. E **63**, 041510 (2001).
[32] D. A. Head, A. J. Levine, and F. C. MacKintosh, Phys. Rev. Lett. **91**, 108102 (2003).
[33] J. Wilhelm and E. Frey, Phys. Rev. Lett. **91**, 108103 (2003).